

LA-UR-98- 3 4 2 3

Los Alamos National Laboratory is operated by the University of California for the United States Department of Energy under contract W-7405-ENG-36

CONF-980803--

TITLE: THERMODYNAMICS AND SOUND SPEEDS AT THE  
CHAPMAN-JOUGUET STATE

AUTHOR: J. N. Fritz and C. A. Forest  
LANL, Los Alamos, NM 87545

SUBMITTED TO: Eleventh International Detonation Symposium  
August 31 - September 4, 1998  
Snowmass, CO

RECEIVED  
APR 13 1999  
OSTI

DISTRIBUTION OF THIS DOCUMENT IS UNLIMITED *ph*

MASTER

By acceptance of this article, the publisher recognizes that the U.S. Government retains a nonexclusive, royalty-free license to publish or reproduce the published form of this contribution, or to allow others to do so, for U.S. Government purposes.

The Los Alamos National Laboratory requests that the publisher identify this article as work performed under the auspices of the U.S. Department of Energy.

Los Alamos

Los Alamos National Laboratory  
Los Alamos, New Mexico 87545

## **DISCLAIMER**

**This report was prepared as an account of work sponsored by an agency of the United States Government. Neither the United States Government nor any agency thereof, nor any of their employees, makes any warranty, express or implied, or assumes any legal liability or responsibility for the accuracy, completeness, or usefulness of any information, apparatus, product, or process disclosed, or represents that its use would not infringe privately owned rights. Reference herein to any specific commercial product, process, or service by trade name, trademark, manufacturer, or otherwise does not necessarily constitute or imply its endorsement, recommendation, or favoring by the United States Government or any agency thereof. The views and opinions of authors expressed herein do not necessarily state or reflect those of the United States Government or any agency thereof.**

## **DISCLAIMER**

**Portions of this document may be illegible in electronic image products. Images are produced from the best available original document.**

# THERMODYNAMICS AND SOUND SPEEDS AT THE CHAPMAN-JOUGUET STATE\*

J. N. Fritz and C. A. Forest  
Los Alamos National Laboratory, Los Alamos, New Mexico, 87545

Some thermodynamic relations about an equilibrium Chapman-Jouguet (CJ) state are obtained. Relations for sound speeds in the wave velocity-particle velocity plane are derived. A relation between the slope of the sound speed in this plane and the asymptotic slope of the Hugoniot is suggested.

## INTRODUCTION

In a previous paper [1] experimental measurements of sound speeds at high pressures were used to determine the Chapman-Jouguet (CJ) state of the plastic-bonded explosive PBX-9501. In this paper we derive some general relations about sound speeds at high pressures, and in particular, some relations between the sound-speed curves and overdriven detonations in the vicinity of the CJ state. Such relations are, of course, implicit in the thermodynamic EOS description of a material and have been touched upon before [2-4]. When an experimental technique becomes active and new results are available, it is appropriate to refine and look more closely at these relations in the variables appropriate to the experiment. We do that here. In section II we review the basic thermodynamics for shocks. In III we obtain the sound speed along the Hugoniot in terms of the Hugoniot and the Grüneisen function and in terms of the CJ isentrope and the Grüneisen function. Special relations at the CJ state are derived. An approximation relating the slope of the sound-speed curve to the asymptotic slope of the

Hugoniot is derived. In IV we apply a few of these relations to the data obtained before [1].

The overdriven Hugoniot for explosives has certain peculiarities in the velocities plane. These peculiarities make many fitting schemes (e.g., a simple polynomial in  $u$ ) ineffective. The exact thermodynamic relations obtained here show the properties that any effective data-fitting scheme must have.

## SHOCK THERMODYNAMICS

The jump conditions for mass and momentum across a shock wave ( $\rho_0 u_s = \rho(u_s - u)$  and  $P - P_0 = \rho_0 u_s u$ ) give pressure and specific volume in terms of the shock and particle velocities. Inverses ( $\rho_0^2 u_s^2 = (P - P_0)/(V_0 - V)$  and  $u^2 = (P - P_0)(V_0 - V)$ ) serve to define the velocities in terms of the Hugoniot locus  $P_h(V)$ . The jump condition for the energy  $E - E_0 = \frac{1}{2}(P + P_0)(V_0 - V)$  together with an  $E(P, V)$  defines the Hugoniot locus in  $P(V)$ . The transformation between  $P(V)$  and  $u_s(u)$  permits description of thermodynamics in the wave velocity-particle velocity plane, a description suited to the measured experimental variables.

If we have some cross-curve  $P_x(V)$  (one where the volume is varying) and we know the energy along this curve (isentropes and Hugoniots are

---

\*This work supported by the U. S. Department of Energy.

two types of curves where the energy is readily obtained), then we can express the energy in the desired  $E(P, V)$  form:

$$E(P, V) = E_x(V) + \int_{P_x(V)}^P dpV/\gamma(p, V), \quad (1)$$

where  $p$  is an integration variable with  $V$  held constant, and  $\gamma = V(\partial P/\partial E)_V$ , the Grüneisen function.

If we have a curve  $P_x(V)$  we define the modulus for that curve as  $B_x = -VdP_x/dV$ . The isentropic bulk-modulus  $B_S$  is related to the velocity  $c$  of a small-amplitude wave in a fluid media by  $B_S = \rho c^2$  [5]. This velocity is with respect to the compressed media at rest. It is convenient to work with the Lagrangian velocity  $L_c = \rho c/\rho_0$ . We have:

$$c^2 = B_S/\rho, \quad L_c^2 = \rho B_S/\rho_0^2. \quad (2)$$

Other moduli will be useful. Along a Hugoniot curve  $P_h(V)$  we define  $B_h = -VdP_h(V)/dV$ . The chord connecting the initial state to the final shocked-state is the Rayleigh line. We define a modulus associated with this slope as  $B_R = V_0(P - P_0)/(V_0 - V) = \rho_0 u_s^2$ . For the chord the choice for the multiplying volume is ambiguous. We also define  $B_{ch} = V(P - P_0)/(V_0 - V) = \rho_0 u_s(u_s - u)$ . This will permit a pleasing symmetry in an equation for the Grüneisen function.

The dimensionless curvature of a  $P_x(V)$  curve is also of interest. If  $B_x = -VP'_x$  (a prime on  $P$  will usually denote a volume derivative), then  $dB_x/dV = -P'_x - VP''_x$ . Alternatively we have  $dB_x/dV = (dP_x/dV)(dB_x/dP) = -(B_x/V)(dB_x/dP)$ . Equating these yields:

$$\frac{V^2 P''_x}{B_x} = 1 + \frac{dB_x}{dP}. \quad (3)$$

The "fundamental derivative"  $\mathcal{G}$  used by Menikoff and Plohr [4] is half of this curvature on an isentrope, i. e.,  $2\mathcal{G} = V^2 P''_S/B_S$ .

Dimensionless forms for the moduli are frequently used. We define  $\gamma_x = B_x/P_x$ . The isentropic gamma

$$\gamma_S = \frac{B_S}{P} = -\left(\frac{\partial \ln P}{\partial \ln V}\right)_S = \frac{\rho c^2}{P}. \quad (4)$$

is a variable frequently used to describe detonation-product isentropes [6].

Following Courant and Friedrichs [5] we use the Hugoniot function  $h(P, V) = E - E_0 - \frac{1}{2}(P + P_0)(V_0 - V)$ . Clearly  $h = 0$  defines  $P_h(V)$ . Other curves with constant- $h$  correspond to Hugoniot with a different energy in the initial state. From the first law and  $TdS(dP, dV)$  we get

$$dh = TdS - \frac{1}{2}(V_0 - V)dP - \frac{1}{2}(P - P_0)dV = \left(\frac{V}{\gamma} - \frac{V_0 - V}{2}\right)dP + \left(\frac{B_S}{\gamma} - \frac{P - P_0}{2}\right)dV. \quad (5)$$

For  $dh = 0$  we obtain

$$-V\left(\frac{\partial P}{\partial V}\right)_h \equiv B_h = \frac{B_S - (\gamma/2)(P - P_0)}{1 - (\gamma/2V)(V_0 - V)}. \quad (6)$$

This equation can be solved for the Grüneisen function:

$$\frac{\gamma}{2V}(V_0 - V) = \frac{B_h - B_S}{B_h - B_{ch}}. \quad (7)$$

These  $B$ 's all have a common  $V$ -factor, so this ratio of differences can also be regarded as the ratio of differences of the slopes of the various curves. Eq. (6) can also be solved for  $B_S$ :

$$B_S = \left\{1 - \left(\frac{\gamma}{2V}\right)(V_0 - V)\right\} B_h + \frac{\gamma}{2}(P - P_0). \quad (8)$$

This, with (2), gives the sound speed *on the Hugoniot*.

For an exothermic Hugoniot (more precisely, for  $h(P_0, V_0) > 0$ ) the "first" solution for a shock is obtained when we raise the Rayleigh line to be tangent to the Hugoniot curve, i. e.,  $B_h = B_{ch}$ . *At the tangent point* we can make the following observations. If we insert this condition in Eq. (8) we find  $B_S = B_{ch}$ . This result in Eq. (2) implies  $L_c = u_s$ . This, combined with the relation between  $L_c$  and  $c$  and the mass jump condition implies  $c = u_s - u$ , the sonic condition. The  $u_s$  at this minimum shock-velocity is denoted by  $D$ , the CJ detonation-velocity. The argument is reversible, the sonic condition implies the triple-tangency between the Hugoniot, Rayleigh line, and isentrope. The usual caveats apply; these results are valid when reaction rates are fast enough to get a close approach to equilibrium.

## SOUND-SPEED RELATIONS

In this paper we are particularly interested in the curves  $L_{ch}(u)$  (the Lagrange sound-speed

along the Hugoniot) and  $u_s(u)$  (the OD Hugoniot) as they extend above the CJ state. As we go higher in pressure we expect reaction rates to be faster, and we expect that measured results will be closer to true equilibrium values. The equilibrium Lagrange sound-speed can be obtained as a functional of the OD Hugoniot and the Grüneisen function with the aid of Eqs. (2) and (8), *i. e.*,  $L_{ch}(u) = f : u_s(u), \gamma$ . These would directly express  $L_c(P, V)$ . We would like it in the  $u_s$ - $u$  plane. The jump conditions and their inverses can be regarded as transformations between these two planes of variables. Differential forms of the transformation

$$-dV/du = V_0(u_s - uu'_s)/u_s^2, \quad (9)$$

$$dP/du = \rho_0(u_s + uu'_s), \quad (10)$$

where  $u'_s = du_s/du$ , can be used to effect the transformation to the velocities plane. An intermediate result, using the definition of  $B_h$ , is

$$B_h = \rho_0 u_s (u_s - u) \frac{u_s + uu'_s}{u_s - uu'_s}. \quad (11)$$

One notes that  $B_h = B_{ch}$  implies  $2uu'_s = 0$ , *i. e.*, you can have this condition at the beginning of the Hugoniot ( $u = 0$ ), or if the tangency occurs for finite  $u$  the slope of the  $u_s(u)$  Hugoniot must be zero. We then have:

$$\left(\frac{L_{ch}}{u_s}\right)^2 = \left\{1 - \left(\frac{\gamma V_0}{2V}\right) \frac{u}{u_s}\right\} \frac{u_s + uu'_s}{u_s - uu'_s} + \left(\frac{\gamma V_0}{2V}\right) \frac{u}{u_s} = G/(u_s - uu'_s), \quad (12)$$

where

$$G = u_s + uu'_s \left\{1 - \left(\frac{\gamma V_0}{V}\right) \frac{u}{u_s}\right\}. \quad (13)$$

We take the logarithm of Eq. (12) and then the derivative to obtain:

$$2 \left(\frac{L'_{ch}}{L_{ch}} - \frac{u'_s}{u_s}\right) = \frac{uu''_s}{u_s - uu'_s} + \frac{G'}{G}, \quad (14)$$

where

$$G' = u'_s + (u'_s + uu''_s) \left\{1 - \left(\frac{\gamma V_0}{V}\right) \frac{u}{u_s}\right\} + uu'_s \left(\frac{u_s - uu'_s}{u_s^2}\right) \frac{\gamma V_0}{V} \left\{\frac{u}{u_s - u} \frac{d \ln(\gamma/V)}{d \ln V_h} - 1\right\}. \quad (15)$$

We expect  $L'_{ch} \equiv dL_{ch}/du$  to be approximately constant over our data range. The complexity of (14) is due to the structure a Hugoniot has when it represents a detonation. We switch quickly from  $u'_s = 0$  and a non-zero curvature at CJ to  $u'_s$  a constant and  $u''_s \approx 0$  in the linear range of the OD Hugoniot. The complicated form for  $L'_{ch}$  is probably required to keep it roughly constant. At the CJ state we have  $u'_s = 0$ ,  $L_c = u_s = G = D$ , and thus:

$$\left(\frac{dL_{ch}}{du}\right)_{cj} = u_{cj} u''_s \left\{1 - \left(\frac{\gamma V_0}{2V}\right)_{cj} \frac{u_{cj}}{D}\right\}. \quad (16)$$

This equation gives a close connection between the slope of our experimental sound-speed and the curvature of the OD Hugoniot at the CJ state. This equation is likely to be used to establish a good value for the curvature rather than the other way around. If a very accurate  $u''_s$  could be obtained from the Hugoniot curve an estimate of  $\gamma$  at the CJ state could be made.

What we would really like is a relation between  $L'_{ch}$  and some other readily measurable EOS parameter, *e. g.*, the asymptotic slope of  $u_s(u)$ . We have concentrated on  $L_{ch}(u) = f : u_s(u), \gamma$ . We may expect a simpler result if we consider  $L_{ch}(u) = f : P_S(V), \gamma$ , where  $P_S(V)$  is the CJ isentrope. It does not have the complications that the Hugoniot does. We do have the additional complication that we follow the sound speed along the Hugoniot experimentally, and not along the isentrope. In Eq. (1) we let the  $x$ -curve be the CJ isentrope. Then with  $E_{cj} - E_0 = \frac{1}{2}(P_{cj} + P_0)(V_{cj} - V_0)$ , and  $E_x = E_{cj} - \int P_S dV$ ; we obtain:

$$\frac{1}{2}(P_h + P_0)(V_0 - V) = \frac{1}{2}(P_{cj} + P_0)(V_0 - V_{cj}) - \int_{V_{cj}}^V dV P_S(V) + \int_{P_S}^{P_h} dp \frac{V}{\gamma(p, V)}, \quad (17)$$

*i. e.*, we have  $P_h = f : P_S, \gamma$ . We take the volume derivative of (17) and rearrange the terms slightly:

$$\frac{-VP'_h}{\gamma_{gh}} \left\{1 - \frac{\gamma_{gh}}{2V}(V_0 - V)\right\} = \frac{1}{2}(P_h + P_0) - P_S - \frac{VP'_S}{\gamma_{gS}} + \int_{P_S}^{P_h} dp \frac{\partial}{\partial V_p} \left(\frac{V}{\gamma(p, V)}\right). \quad (18)$$

This combines with (8) to yield:

$$\frac{B_S(P_h, V)}{\gamma_{gh}} = \frac{B_S(P_S, V)}{\gamma_{gS}} + (P_h - P_S) + \int_{P_S}^{P_h} dp \frac{\partial}{\partial V_p} \left( \frac{V}{\gamma(p, V)} \right). \quad (19)$$

We note that this equation is the integral form of the Maxwell relation,  $(\partial(B_S/\gamma - P)/\partial P)_V = (\partial(V/\gamma)/\partial V)_P$ . It does not depend on the  $P$ 's being on particular curves; any two pressures would do. Combined with Eq. (2) it does give us the sound speed along the Hugoniot in terms of the sound speed along the isentrope plus a term proportional to the offset  $P_h - P_S$ . We have a slowly-varying major term and a linearly-increasing minor term which combine (in view of the experimental result) to give a linear variation of sound speed with velocity. This is in contrast to Eq. (14) where both  $u'_s$  and  $u''_s$  are major players and switch roles as we move from the CJ state to an asymptotic linear  $u_s(u)$ . We then have:

$$L_{c_h}^2 = \frac{\rho \gamma_{gh}}{\rho_0^2} \left\{ \frac{B_S(P_S, V)}{\gamma_{gS}} + (P_h - P_S) + \int_{P_S}^{P_h} dp \frac{\partial}{\partial V_p} \left( \frac{V}{\gamma(p, V)} \right) \right\}. \quad (20)$$

We could write down the complete equation for  $L_{c_h}^2$  by introducing a lot of  $\gamma$ -derivatives, but this is not particularly illuminating. We concentrate on the derivative at the CJ state. There, any term with  $P_h - P_S$  or  $P'_h - P'_S$  as a factor will vanish because of the coincidence and tangency of the isentrope and Hugoniot. The derivative of  $\gamma_{gh}/\gamma_{gS}$  has a factor  $P'_h - P'_S$ . The only term contributing is  $\rho B_S = -P'_S$ . Then we use  $L_{c_h}^2 = (dV/du)(d^L c_h/dV)$ . From Eq. (9) and the jump conditions we have:

$$\frac{dV}{du} = \frac{2\sqrt{(P_h - P_0)(V_0 - V)}}{P'_h(V_0 - V) - (P_h - P_0)} = -\frac{2V\rho_0 u_s}{B_h + B_{ch}}. \quad (21)$$

We obtain at the CJ state (freely using  $L_c = u_s = D$  and  $B_h = B_{ch} = B_S$ ):

$$2^L L_{c_h}^2 = (V_0/V) \frac{V^2 P''_S}{B_S} = \left( \frac{V_0}{V} \right) \left( 1 + \frac{dB_S}{dP} \right). \quad (22)$$

Eq. (18) retains an explicit connection between the isentrope and Hugoniot that we lost in going

to (19). If we take the volume derivative of (18) and use the simplifications at CJ we get a simple relation between the second derivatives of the isentrope and Hugoniot at the CJ state:

$$P''_h = P''_S / \left\{ 1 - \frac{\gamma}{2V}(V_0 - V) \right\}. \quad (23)$$

From the volume derivative of  $u_s^2(P, V)$  we obtain the general equation:

$$u'_s(u) = \frac{V_0 (P'_h + (P_h - P_0)/(V_0 - V))}{P'_h(V_0 - V) - (P_h - P_0)} = \frac{V_0}{V_0 - V} \frac{B_h - B_{ch}}{B_h + B_{ch}}. \quad (24)$$

A linear  $u_s(u)$ , where  $u'_s = s$ , a constant, describes many inert materials. This is clearly not the case for a OD Hugoniot, where  $B_h = B_{ch}$  at CJ and  $u'_s = 0$  there; and then increases to an asymptotic value for the high-pressure range. Another volume derivative yields:

$$uu''_s = \frac{(\rho/\rho_0)B_{ch}}{(B_h + B_{ch})^3} \left\{ 4B_{ch}V^2 P''_h - \frac{2V}{V_0 - V}(B_h - B_{ch})(3B_h + B_{ch}) \right\}. \quad (25)$$

At CJ this reduces to:

$$uu''_s = \frac{\rho}{2\rho_0} \frac{V^2 P''_h}{B_{ch}}. \quad (26)$$

This, in (16), with the aid of (23) and (3) again leads to (22).

For a linear  $u_s(u)$ ,  $\eta \equiv 1 - V/V_0 = u_p/u_s$ , we have  $P_h = \rho_0 c_0^2 \eta / (1 - s\eta)^2$ , and we can evaluate  $1 + dB_h/dP$ , a measure of the curvature  $P''_h(V)$  as:

$$1 + \frac{dB_h}{dP} = 4s \frac{(1 + s\eta/2)(1 - \eta)}{(1 + s\eta)(1 - s\eta)}. \quad (27)$$

This "curvature" has the value  $4s$  times a slowly-varying function of  $\eta$ . At the centering point  $1 + dB_h/dP = 1 + dB_S/dP$  because of the second-order contact between the isentrope and Hugoniot. A linear  $u_s(u)$ , an initial porous-state, and an appropriate Grüneisen function works well (the snowplow model) for many materials, at least for higher pressures. In the high-pressure range the  $u_s(u)$  for the porous media asymptotes to a

line slightly below and parallel (*i. e.*, the same  $s$ ) to the linear  $u_s(u)$  for the solid material. A similar description is possible for an OD Hugoniot; one changes the  $E_0$  for the centering point from its regular thermodynamic value just as one changed  $V_0$  to represent a porous material. The OD Hugoniot would then asymptote to the base linear Hugoniot from above. Setting  $1 + dB/dP$  constant is the basis for the Murnaghan family of equations of state. If this quantity is constant for detonation products and the reverse "snowplow" model is valid, the following relation is suggested between the slope of the measured sound-speed and the asymptotic  $s$  of the OD Hugoniot:

$${}^L c'_h \approx 2s(V_0/V)_{cj}. \quad (28)$$

We consider the relation between the slope of  $c + u$  and  ${}^L c$ . From  $c = (\rho_0/\rho){}^L c = (1 - u/u_s){}^L c$  we obtain:

$$\frac{d(c+u)}{du} = 1 - \frac{u_s - uu'_s}{u_s^2} {}^L c + \frac{\rho_0}{\rho} \frac{d{}^L c}{du}. \quad (29)$$

At CJ this reduces to

$$\frac{d(c+u)}{du} = \frac{\rho_0}{\rho} \frac{d{}^L c}{du} = \frac{1}{2} \left( 1 + \frac{dB_S}{dP} \right) \approx 2s. \quad (30)$$

#### APPLICATION TO THE DATA

In the previous paper [1] an analytic form was chosen to represent the overdriven Hugoniot of PBX-9501. An alternative approach is to have a running local fit to the data with a level of smoothing compatible with the precision of the data. A tabular function (briefly described in Appendix A) is used to fit the detonation-Hugoniot data with particle velocities greater than the particle velocity of the CJ state. The slope  $u'_s$  of the tabular function was set equal to zero at the  $u_{pCJ}$  from the analytic fit, but the detonation velocity was allowed to vary. The tabular function representing the slope of the detonation Hugoniot is presented in Fig. 1.

The characteristic shape of the PBX-9501 detonation Hugoniot is graphically displayed in this figure. The slope is zero at the CJ state and monotonically increases with increasing particle velocity. The slope linearly increases near the CJ state and then gradually flattens out at larger particle velocities to essentially a maximum slope.

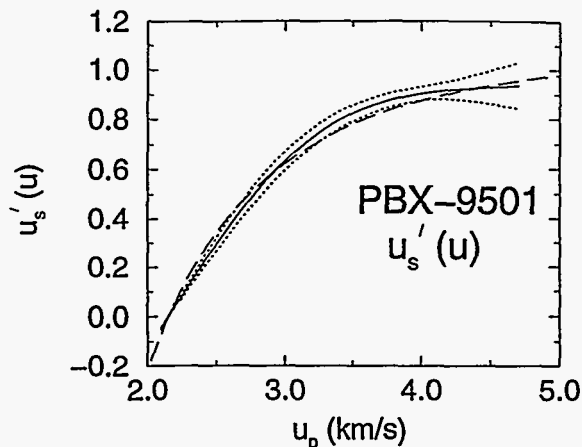


FIGURE 1. The slope  $u'_s(u)$  (solid line) from local running fits. The dotted lines indicate error limits. The dashed line is the slope from the previous analytical fit.

The general shape of  $u'_s$  is common to other detonation Hugoniots we have studied (Composition B, PBX-9502, and TNT). However, for some of these explosives the maximum asymptotic slope was not attained over the particle-velocity range investigated. For these explosives there was still a small non-zero slope to  $u'_s(u)$  at large particle velocities.

The dashed lines above and below the fitted curve represent the two-sigma error limits at the 95% probability limit. The error limits are close together at the CJ state, because of the slope constraint, and gradually increase at intermediate particle velocities. The large error limits at the end of the data range occur because central centered differences can no longer be taken over the usual interval. The other curve in Fig. 1 is the slope of the analytic fit obtained in the previous paper. If error limits were placed on this curve, a satisfactory overlap of the methods of fitting would be obtained.

From the figure we estimate an asymptotic slope for the OD Hugoniot of  $0.95 \pm 0.10$ . The RHS of the approximate relation Eq. (28) then (with our best estimate for the CJ state) predicts  $2.50 \pm 0.3$  for  ${}^L c'_h(u)$ . The inferred slope 2.712 [1] falls within this range.

Eq. (22) can be combined with Menikoff and Plohr's definition of the derivative  $\mathcal{G}$  to yield:

$${}^L c'_{cj} = (V_0/V_{cj}) \mathcal{G}_{cj}. \quad (31)$$

The slope of the sound-speed curve is closely re-



lated to their fundamental derivative, and the measured  $L'_c(u)$  implies  $G_{cj} = 2.05$ . This value implies a non-pathological concave-upward curve for the CJ isentrope.

In the previous data fitting we were able to choose analytical forms that adequately represented the data. This just means the data doesn't uniquely specify a particular functional form. However, we do recommend that any functional form chosen duplicates the  $u'_s$  shape given in Fig. 1. This insures that both  $u_s$  and  $u'_s$  are smooth continuous functions, which are necessary constraints to obtain thermodynamic variables that are well behaved.

In Fig. 2 the second derivative of the detonation Hugoniot is given. The tabular function code

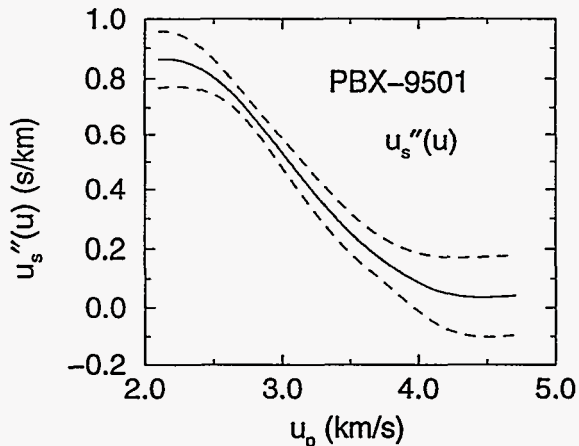


FIGURE 2. The derivative  $u''_s(u)$  from the running fits. Error limits are shown.

was also used to calculate this curve. The curvature is a maximum at the CJ state and monotonically decreases to zero at the end of the data range. The two-sigma error limits are also shown and have the usual behavior at the constrained and unconstrained end points. The exact relation (Eq. (16)) gives  $u''_s = 1.36 \text{ s/km}$  at CJ. This is considerably larger than the  $0.87 \pm 0.1$  value indicated on the graph. This is not too surprising. There weren't a lot of points in the vicinity of the CJ state measuring the curvature.

The high value for the curvature at the CJ state from Eq. (16) and the following measured smooth behavior of the Hugoniot imply difficulties in fitting the Hugoniot with some smooth polynomial. The analytic fit previously used [1] probably matches  $u_s(u)$  at the CJ state, but does not match the detailed behavior of  $u'_s(u)$  and  $u''_s(u)$

mandated by these thermodynamic relations.

## CONCLUSIONS

The PBX-9501 overdriven-detonation and sound-speed data is smooth and relatively featureless. Many smooth functions exist that can represent such smooth data. The functions must satisfy the conditions imposed by the Chapman-Jouguet conditions. Further restrictions come from imposing reasonable extrapolation conditions on the functions.

In this paper a tabular function was used to fit the experimental detonation Hugoniot data. An interesting functional form for the derivative  $u'_s(u)$  of the detonation Hugoniot was observed, mainly a derivative that's zero at the CJ state and monotonically increases with increasing particle velocity until a constant maximum value is attained. The measured Lagrange sound-velocities displayed a linear dependence with increasing particle velocity.

Eq. (28) can be used to estimate the sound speed for experimental design purposes, and, in the absence of experimental data, should give a reasonable approximation for the sound speed in the reacted products of a detonation. The near-validity of Eq. (28) and the linearity of the measured Lagrange sound-velocities suggests that EOS models with relatively constant curvature (Murnaghan EOS's, linear  $u_s-u_p$ ) might also describe detonation products very well. The linear base curve would have to be lower in the  $u_s-u_p$  plane than the OD Hugoniot. The variations that  $u'_s$  goes through on the OD Hugoniot would have to be achieved through an initial energy offset (*i. e.*, the "reverse snowplow" model discussed previously).

## APPENDIX: DATA FITTING WITH A TABULAR FUNCTION

Least-squares fitting of data is often done by assuming a particular functional form and optimizing with respect to its parameters. In examining a property of the determined function (such as its derivative) it may be unclear whether the property is strongly related to the data or is principally a result of the assumed functional form. To circumvent this uncertainty, least-squares can be done with functions that have no particular functional form, for instance cubic splines are commonly used. Another choice, which is used here,

is to represent the fitting function as a uniformly-spaced table which is interpolated by a local cubic Lagrange polynomial. The functional values of the table are then the parameters of the fitting function. Smoothness of the fitting function is induced by adding to the merit function a weighted sum of squares of the  $n^{\text{th}}$  order forward-difference operator over the domain of the table. Let  $\{x_i, y_i\}$  be the data set and  $\{t_i, f_i\}$  be the table where  $t_i$  are uniformly spaced over the interval  $\min\{x_i\}$  to  $\max\{x_i\}$ . Let  $F(x)$  be the local central-interval cubic Lagrange interpolation polynomial for the table  $\{t_i, f_i\}$ . Then the merit function for optimization is:

$$\mathcal{E} = \sum_{i=1}^{n_{\text{data}}} (F(x_i) - y_i)^2 + wt \sum_{i=1}^{m_{\text{table}}} (\Delta^n f_i)^2. \quad (\text{A1})$$

The normal equations are then:

$$\frac{\partial \mathcal{E}}{\partial f_i} = 0, \quad \text{for } i = 1, m_{\text{table}}. \quad (\text{A2})$$

Because the optimizing parameters are the  $f_i$ 's, which are local function-values and thereby are directly associated with the residuals of the least-squares, the so determined function is highly dominated by the data and gives residuals randomly distributed about zero. For our particular application we had 20 tabular values uniformly covering the data ( $m_{\text{table}} = 20$ ), a third order smoothing operator ( $n = 3$ ), and a value for  $wt$  that gave an effective weight of 2 for the second term relative to the first term.

The derivative table  $\{t_i, f_i'\}$  is calculated from the  $\{t_i, f_i\}$  table by using a running 4<sup>th</sup>-degree polynomial about central points. A table  $\{t_i, f_i''\}$  is constructed similarly from  $\{t_i, f_i'\}$ .

## REFERENCES

- [1.] J. N. Fritz, R. S. Hixson, M. S. Shaw, C. E. Morris, and R. G. McQueen. Overdriven-detonation and sound-speed measurements in PBX-9501 and the "thermodynamic" Chapman-Jouget pressure. *J. Appl. Phys.*, 80(11):6129-6141, December 1996.
- [2.] R. G. McQueen, S. P. Marsh, J. W. Taylor, J. N. Fritz, and W. J. Carter. The equation of state of solids from shock wave studies. In Ray Kinslow, editor, *High-Velocity Impact Phenomena*, chapter 7. Academic Press, New York, New York, 1970.
- [3.] W. C. Davis. Equation of state for detonation products. In James M. Short, editor, *Eighth Symposium (International) on DETONATION*, pages 119-130, White Oak, Maryland, July 1985. Office of Naval Research NSWC MP 86-194, Naval Surface Weapons Center.
- [4.] Ralph Menikoff and Bradley J. Plohr. The Riemann problem for fluid flow of real materials. *Rev. Mod. Phys.*, 61(1):75-130, January 1989.
- [5.] R. Courant and K. O. Friedrichs. *Supersonic Flow and Shock Waves*. Pure and Applied Mathematics. Interscience Publishers, Inc., New York, New York, 1948.
- [6.] Unfortunately this variable is frequently denoted as a bare  $\gamma$ , the same symbol we use for the Grüneisen function. We shall always use the subscript form. Sometimes a subscripted  $\gamma$  is used to denote the Grüneisen function along a particular path. We will use a functional notation to denote this case, e. g.,  $\gamma(P_h(V), V)$  for  $\gamma$  along a Hugoniot. As an alternative to this we'll occasionally use  $\gamma_{gh} = \gamma(P_h, V)$ , etc.